Lattice dynamics and electron-phonon coupling in the β-$(BEDT\text{-}TTF)_2I_3$ organic superconductor

Alberto Girlando, Matteo Masino, and Giovanni Visentini
Dipartimento di Chimica Generale ed Inorganica, Chimica Analitica, Chimica Fisica, Università di Parma, Parco Area delle Scienze, I-43100 Parma, Italy

Raffaele Guido Della Valle, Aldo Brillante, and Elisabetta Venuti
Dipartimento di Chimica Fisica e Inorganica, Università di Bologna, Viale Risorgimento 4, I-40136 Bologna, Italy
(Received 17 March 2000; revised manuscript received 9 June 2000)

The crystal structure and lattice phonons of the $(BEDT\text{-}TTF)_2I_3$ superconducting β phase (where BEDT-TTF is bis-ethylen-dithio-tetrathiafulvalene) are computed and analyzed by the quasiharmonic lattice dynamics (QHLD) method. The empirical atom-atom potential is that successfully employed for neutral BEDT-TTF and for nonsuperconducting α-$(BEDT\text{-}TTF)_2I_3$. The rigid molecule approximation has to be relaxed by allowing mixing between lattice and low-frequency intramolecular vibrations. Such a mixing is found to be essential to account for the specific heat measurements, and also yields good agreement with the observed Raman and infrared frequencies. The crystal structure and its temperature and pressure dependence are also properly reproduced, though the effect of the mixing is less important in this case. From the eigenvectors of the low-frequency phonons we calculate the electron-phonon coupling constants due to the modulation of charge transfer (hopping) integrals. The charge transfer integrals are evaluated by the extended Hückel method applied to all nearest-neighbor BEDT-TTF pairs in the *ab* crystal plane. From the averaged electron-phonon coupling constants and the QHLD phonon density of states we derive the Eliashberg coupling function $\alpha^2(\omega)F(\omega)$, which compares well with that experimentally obtained from point contact spectroscopy. The corresponding dimensionless coupling constant λ is found to be ~ 0.4.

I. INTRODUCTION

The strength and importance of electron-lattice phonon (*e-lph*) coupling in the superconductivity mechanism of organic superconductors has always been rather controversial. Early numerical estimates based on simplified models gave very low values for the coupling to acoustic phonons,[1] and much more attention was then devoted to electron-molecular vibration (*e-mv*) coupling.[2] On the other hand, ''librons'' were also invoked in the pairing mechanism of organic superconductors.[3,4] On the experimental side, most of the data have been collected for bis-ethylen-dithio-tetrathiafulvalene (BEDT-TTF) salts, which are the most extensive and representative class of organic superconductors.[5] In particular, recent Raman experiments on BEDT-TTF salts pointed out that the intensity[6] and the frequency[7] of some low-frequency phonon modes change at the superconducting critical temperature T_c. Oddly enough, also one intramolecular BEDT-TTF mode has been shown to exhibit a frequency shift at T_c.[8] Carbon isotopic substitution on the central double bond BEDT-TTF was claimed to have dramatic effects on the T_c of one superconducting BEDT-TTF salt,[9] but subsequent extensive isotopic substitution studies on other superconducting BEDT-TTF salts strongly suggested that the lattice phonons are likely involved in the superconducting mechanism.[10] Attempts to take into account both *e-mv* and *e-lph* coupling have been put forward,[11] but the role and the relative importance of the two types of coupling in the pairing mechanism is far from being settled.

Whereas extensive studies have been devoted to the characterization of intramolecular phonons of BEDT-TTF (Refs. 12–14) and to the estimate of the relevant *e-mv* coupling strength,[15] very little is known about the lattice phonon structure in BEDT-TTF salts or in other organic superconductors. Obtaining a sound characterization of BEDT-TTF salts lattice phonons is not easy, since in general the unit cell contains several molecular units, and the phonon modes obviously differ for different crystalline structures. We have tackled the problem by adopting the ''quasiharmonic lattice dynamics'' (QHLD) method,[16,17] by which we are able to analyze both the crystal and the lattice phonon structure in terms of empirical atom-atom potentials. Potentials of this kind have been found to be very successful in describing molecular and ionic-molecular crystals,[18] and are reasonably transferable among crystals containing the same atoms. We have first obtained C, S, and H atom-atom potential parameters reproducing crystal structure and lattice phonons of neutral BEDT-TTF.[19] Then we have considered the I_3^- salts, which have only one additional atom to parametrize, and present several crystalline phases.[5] After the successful application of the potential to the nonsuperconducting α-$(BEDT\text{-}TTF)_2I_3$ crystal,[20] we present in this paper the results relevant to the extensively studied superconducting β phases.

β-$(BEDT\text{-}TTF)_2I_3$ was the first ambient pressure BEDT-TTF based superconductor to be discovered,[21] and its unit cell contains only one formula unit.[22] The BEDT-TTF radicals are arranged in stacks, and the stacks form sheets parallel to the *ab* crystal plane. The centrosymmetric linear I_3^- anions separate the sheets, forming an insulating layer. Several variants of the β-$(BEDT\text{-}TTF)_2I_3$ phase have been reported, making difficult a full and detailed characterization. The electrochemically prepared β-$(BEDT\text{-}TTF)_2I_3$ exhibits ambient pressure superconductivity at $T_c = 1.3$ K [β_L-

$(BEDT\text{-}TTF)_2I_3$] or at $T_c=8.1$ [β_H- or β^*-$(BEDT\text{-}TTF)_2I_3$] depending on the pressure-temperature history of the sample. Such T_c increase has been attributed to a pressure induced ordering process of the ethylene groups of the BEDT-TTF cation.[23] In addition, thermal treatment or laser irradiation of the α-phase yields an irreversible transformation to a superconducting phase ($T_c=8.0$ K), named α_t-$(BEDT\text{-}TTF)_2I_3$,[6] which was claimed to be similar to the β phase. On the other hand, β-$(BEDT\text{-}TTF)_2I_3$ can also be prepared by direct chemical oxidation [β_{CO}-$(BEDT\text{-}TTF)_2I_3$],[24] with T_c between 7.1 and 7.8 K. Recent x-ray data confirm that thermally treated α-$(BEDT\text{-}TTF)_2I_3$ is identical to β_{CO}-$(BEDT\text{-}TTF)_2I_3$,[25] but it is still not clear whether β_{CO}-$(BEDT\text{-}TTF)_2I_3$ is the same as β_H-$(BEDT\text{-}TTF)_2I_3$: the possibility of non-stoichiometric phases has also been put forward as an alternative to the ordering process in causing a T_c of about 8 K.[26]

The paper is organized as follows. We first discuss in some detail the methods we have adopted to calculate the structure, the phonon dynamics and the *e-lph* coupling strength of β-$(BEDT\text{-}TTF)_2I_3$ salts. The results are then presented and compared with available experimental data. Finally, the possible role of low frequency phonons in the pairing mechanism of organic superconductors is briefly discussed.

II. METHODS

A. Quasiharmonic lattice dynamics

The crystal structure at thermodynamic equilibrium of $(BEDT\text{-}TTF)_2I_3$ salts is computed using quasiharmonic lattice dynamics (QHLD). In QHLD[16,17] the Gibbs free energy $G(p,T)$ of the crystal is approximated with the free energy of the harmonic phonons calculated at the average lattice structure ($\hbar=1$):

$$G(p,T)=\Phi_{\text{inter}}+pV+\sum_{\mathbf{q}i}\frac{\omega_{\mathbf{q}i}}{2}+k_BT\sum_{\mathbf{q}i}\ln\left[1-\exp\left(-\frac{\omega_{\mathbf{q}i}}{k_BT}\right)\right]. \quad (1)$$

Here, Φ_{inter} is the total potential energy of the crystal, pV is the pressure-volume term, $\Sigma_{\mathbf{q}i}\omega_{\mathbf{q}i}/2$ is the zero-point energy, and the last term is the entropic contribution. The sums are extended to all phonon modes of wave vector $\mathbf{q}$ and frequency $\omega_{\mathbf{q}i}$. Given an initial lattice structure, one computes Φ_{inter} and its second derivatives with respect to the displacements of the molecular coordinates. The second derivatives form the dynamical matrix, which is numerically diagonalized to obtain the phonon frequencies $\omega_{\mathbf{q}i}$ and the corresponding eigenvectors. The structure as a function of p and T is then determined self-consistently by minimizing $G(p,T)$ with respect to lattice parameters, molecular positions and orientations.

In the case of $(BEDT\text{-}TTF)_2I_3$ salts, and in particular of the β phase, the choice of the initial lattice structure is somewhat problematic, due to the conformational disorder of the BEDT-TTF molecules. In fact, the x-ray structural investigations[27] indicate that β-$(BEDT\text{-}TTF)_2I_3$ at 120 K is disordered with two alternative sites for the terminal C atoms, labeled 9a,10a (staggered form) and 9b,10b (eclipsed form). On the other hand, *ab initio* calculations[28] for neutral BEDT-TTF indicate that the ''boat'' geometry (C_2 symmetry) is more stable than the ''planar'' geometry (D_2 symmetry) by 0.65 kcal/mole. The ''chair'' distortion (C_s symmetry) is slightly more stable than the planar molecule, but still less stable than the boat one. The $BEDT\text{-}TTF^+$ ion is planar, and in $(BEDT\text{-}TTF)_2I_3$ crystals we have a statistical mixture of neutral and ionized molecules. On the basis of the site symmetry constraints, we observe that neutral molecule boat and chair geometries correspond to the Leung's configurations 9a,10a and 9b,10b, respectively.[27] Thus the conformational disorder observed in most BEDT-TTF salts is readily understood: the energetic cost of deforming the molecules is small with respect to the energy gain among different packing arrangements in the crystals. To investigate at least partially the effect of conformational disorder on the stability of $(BEDT\text{-}TTF)_2I_3$ phases, we have performed several calculations starting from different initials molecular geometries, as detailed in Sec. III.

TABLE I. Parameters for the atom-atom potential $V_{ij}(r)=A_{ij}\exp(-B_{ij}r)-C_{ij}/r^6$. V is in kcal/mol, r in Å, A,B,C in consistent units. Heteroatom parameters are given by $A_{ij}=\sqrt{A_{ii}A_{jj}}$, $B_{ij}=(B_{ii}+B_{jj})/2$ and $C_{ij}=\sqrt{C_{ii}C_{jj}}$.

i	A_{ii}	B_{ii}	C_{ii}
H	2868	3.74	40.2
C	71460	3.60	449.3
S	329600	3.31	5392.0
I	642376	3.09	16482.6

B. Potential model

We have adopted a pairwise additive intermolecular potential of the form $\Phi_{\text{inter}}=\frac{1}{2}\Sigma_{mn}[q_mq_n/r_{mn}+A_{mn}\exp(-B_{mn}r_{mn})-C_{mn}/r_{mn}^6]$ where the sum is extended to all distances r_{mn} between pairs m,n of atoms in different molecules. The Ewald's method[29] is used to accelerate the convergence of the Coulombic interactions q_mq_n/r_{mn}. The atomic charges q_m relevant to $BEDT\text{-}TTF^{0.5+}$ are directly taken from the PDQ (PS-GVB) results of a recent *ab initio* Hartree-Fock calculations.[30] The parameters A_{mn}, B_{mn}, and C_{mn} involving C, H, and S atoms are taken from our previous calculation of neutral BEDT-TTF.[19] Since in the chosen model[31] C-H parameters are computed from C-C and H-H parameters via ''mixing rules,'' the same procedure is adopted here for all the interactions between different types of atoms. The iodine parameters have been derived from 9,10-diiodoanthracene, and successfully tested on α-$(BEDT\text{-}TTF)_2I_3$.[20] The complete atom-atom model is given in Table I.

C. Specific heat

The constant volume specific heat as a function of T is computed directly from its statistical mechanics expression for a system of phonons

$$C_V(T)=\sum_{\mathbf{q}i} k_B\left(\frac{\omega_{\mathbf{q}i}}{k_BT}\right)^2 \exp\left(-\frac{\omega_{\mathbf{q}i}}{k_BT}\right)\left[1-\exp\left(-\frac{\omega_{\mathbf{q}i}}{k_BT}\right)\right]^{-2}. \quad (2)$$

As usual in these cases, Eq. (2) is evaluated by sampling a large number of $\mathbf{q}$ vectors in the first Brillouin zone (BZ).

In our first attempts to compute C_V, we sampled over regular grids in the BZ. We have found that for $T \leqslant 5$ K the statistical noise was still noticeable even after summing over several thousands of $\mathbf{q}$ vectors; the results were dependent on the sample size. At large T, on the contrary, statistical convergence was quite fast. This pathology can be attributed to the fact that, due to the exponential factor in Eq. (2), only the phonons with $\omega_{\mathbf{q}i} \leqslant k_BT$ give a non-negligible contribution to $C_V(T)$. For very low T, only the acoustic branches of the phonons with $\mathbf{q}$ close to zero have sufficiently small frequencies. With a regular grid, only a few of these vectors are sampled, and most of the computer time is wasted over regions of the BZ that are already well sampled.

To obtain accurate statistics at a reasonable cost, we have used a Monte Carlo (random) integration scheme, biased to yield a larger sampling probability close to $\mathbf{q}=0$. For computational simplicity, we have chosen a three-dimensional Lorentzian probability distribution $L(\mathbf{q}) \propto (1+a|\mathbf{q}|^2)^{-1}$, where a is a width parameter. The bias is compensated by using the reciprocal of the sampling probability as the sample weight. With this scheme most of the computer effort is spent in the region $\mathbf{q} \approx 0$, where a denser sampling really matters. By summing over about 2000 $\mathbf{q}$ vectors, we have been able to reach a satisfactory statistical convergence in the whole range between 0.1 and 20 K. At high T, the results coincide with those obtained by integrating over a grid. At low T, C_V goes as T^3, as it should when the acoustic modes are properly sampled, and does not fluctuate with the sample size.

D. Coupling with low-frequency intramolecular degrees of freedom

In most calculations for molecular crystals all intramolecular degrees of freedom are neglected and the molecules are maintained as rigid units. This rigid molecule approximation (RMA) is reasonable for small compact molecules, like benzene, where all normal modes have frequencies much higher than those of the lattice phonons.

Since for both I_3^- and BEDT-TTF several investigations[13,14,32] suggest that there are low frequency intramolecular modes, the validity of RMA for $(BEDT\text{-}TTF)_2I_3$ appears questionable. Therefore, we have decided to relax the RMA and to investigate the effects of the intramolecular degrees of freedom. For this purpose we adopt an excitonlike model.[29] To start with, it is convenient to use a set of molecular coordinates Q_i describing translations, rotations, and internal vibrations of the molecular units in the crystal. To each BEDT-TTF molecule of $N=26$ atoms we associate the following $3N$ coordinates: three mass-weighted Cartesian displacements of the center of mass, three inertia-weighted rotations about the principal axes of inertia, and $3N-6=72$ internal vibrations (the normal modes of the isolated BEDT-TTF molecule). The I_3^- ion, which is linear, has three translations, two rotations, and four internal vibrations. In order to compute the phonon frequencies, we need all derivatives $\partial^2\Phi/\partial Q_{ri}\partial Q_{sj}$ of the total potential Φ with respect to all pairs of molecular coordinates Q_{ri} and Q_{sj}. Here r and s label molecules in the crystal, while i and j distinguish molecular coordinates.

The potential Φ is made of intramolecular and intermolecular parts Φ_{intra} and Φ_{inter}. In the exciton model, the diagonal derivatives of Φ_{intra} potential are taken to coincide with those of an isolated molecule: $\partial^2\Phi_{\text{intra}}/\partial Q_{ri}^2=\omega_{ri}^2$. Here ω_{ri} is the frequency of the ith normal mode of the rth molecule. All off-diagonal derivatives are zero, which means no coupling among different normal modes, and no coupling between normal modes and rigid rototranslations. These assumptions are correct for the intramolecular potential at the harmonic level (by definition).

The coupling between the molecular coordinates is given by Φ_{inter}. For β-$(BEDT\text{-}TTF)_2I_3$, Φ_{inter} is described by atom-atom and charge-charge interactions, which are both functions only of the interatomic distance. Since the distance depends on the Cartesian coordinates of the atoms X_{ra} the derivatives of Φ_{inter} can be directly computed in terms of the coordinates X_{ra}, and then converted to molecular coordinates Q_{ri}:

$$\frac{\partial^2\Phi_{\text{inter}}}{\partial Q_{ri}\partial Q_{sj}}=\sum_{ab}\frac{\partial^2\Phi_{\text{inter}}}{\partial X_{ra}\partial X_{sb}}\frac{\partial X_{ra}}{\partial Q_{ri}}\frac{\partial X_{sb}}{\partial Q_{sj}}. \quad (3)$$

Here a and b label the Cartesian coordinates of the atoms in molecules r and s, respectively, and the matrix $\partial X_{pa}/\partial Q_{pi}$ describes the Cartesian displacements which correspond to each molecular coordinate Q_{pi}. The displacements corresponding to rigid translations and rotations of the molecules can be derived by simple geometric arguments.[29] The displacements associated to the intramolecular degrees of freedom are the Cartesian eigenvectors of the normal modes of the isolated molecule. The atomic displacements, together with the intermolecular potential model, determine the coupling between intramolecular and lattice modes. We remark that the intramolecular degrees of freedom are taken into account only as far as their effects on the vibrational contribution to the free energy are concerned. No attempt to decrease the potential energy by deforming the molecules is done.

The above mentioned *ab initio* calculations,[13,14] indicating the presence of several low frequency BEDT-TTF intramolecular normal modes, constitute a very convenient starting point for relaxing RMA in QHLD calculations. We include the lowest nine BEDT-TTF internal modes which fall in the same spectral region as the lattice modes (below ~ 220 cm^{-1}),[14] and therefore are likely coupled to lattice phonons. In addition, the symmetric and antisymmetric stretchings, and the two bendings of I_3^-, expected at 114, 145, 52, and 52 cm^{-1}, respectively,[41] have been included in the QHLD calculations. The needed *ab initio* Cartesian displacements of BEDT-TTF were kindly sent us by Liu,[42] while those of I_3^- could be determined by symmetry alone, as often it happens for small molecules with high symmetry.

E. *e-lph* coupling constants and the Eliashberg function

In molecular crystals, intramolecular vibrations are assumed to couple with electrons through modulation of on-

site energies (*e-mv* coupling). Lattice phonons are instead expected to modulate mainly the intermolecular charge transfer (CT) integral, *t*, the corresponding linear *e-lph* coupling constants being defined as

$$g(KL;\mathbf{q},j)=(\partial t_{KL}/\partial Q_{\mathbf{q}j}), \tag{4}$$

where t_{KL} is the CT integral between neighboring pairs K,L of BEDT-TTF molecules, and where $Q_{\mathbf{q}j}$ is the dimensionless normal coordinate for the jth phonon with wave vector $\mathbf{q}$. By relaxing the RMA, as explained above, the distinction between low-frequency intramolecular modes and lattice modes is at least partially lost. On the other hand, *e-mv* coupling by the low-frequency molecular modes is expected to be fairly small, as suggested by the calculations available for isolated BEDT-TTF.[13,14] Therefore, we have assumed that the calculated low-frequency phonons of β-(BEDT-TTF)$_2$I$_3$, occurring between 0 and about 200 cm^{-1}, are coupled to the CT electrons only through the *t* modulation.

To evaluate the $g(KL;\mathbf{q},j)$'s, we have followed a real space approach. Adopting the extended Hückel (EH) method, for each pair K,L of BEDT-TTF molecules within the β-(BEDT-TTF)$_2$I$_3$ crystal we have calculated t_{KL} as the variation of the HOMO energy in going from the monomer to the dimer. Such an approach is known to give *t* values in nice agreement with those calculated by extended basis set *ab initio* methods.[33] t_{KL} is calculated for the dimer equilibrium geometry within the crystal, as well as for geometries displaced along the QHLD eigenvectors. The various $g(KL;\mathbf{q},j)$ are then obtained by numerical differentiation. We have considered only the modulation of the four largest *t*'s, all lying on the *ab* crystal plane.

In the case of *e-mv* coupling the overall electron-phonon coupling strength is generally expressed by the small polaron binding energy, $E_{sp}^{mv}=\Sigma_i g_i^2/\omega_i$, where both g_i, the ith *e-mv* coupling constant, and ω_i, the corresponding reference frequency, are quite naturally taken as independent of the wave vector $\mathbf{q}$.[15] Also in the calculation of the *e-lph* coupling we have assumed the optical lattice phonons as dispersionless, and have performed the calculations for the $\mathbf{q}=0$ eigenvectors only. Within this approximation, symmetry arguments show that only the totally symmetric (A_g) phonons can be coupled with electrons. Thus, the overall *e-lph* coupling strength for the jth lattice *optical* phonon can again be expressed by the small polaron binding energy relevant to that phonon: $\epsilon_j=\Sigma_{KL}(g_{KL,j}^2/\omega_j)$. The total coupling strength is then given by $E_{sp}^{lp}=\Sigma_j\epsilon_j$.

For the three acoustic branches we must of course consider the $\mathbf{q}$ dependence of the g's, the coupling constants being zero for $\mathbf{q}=0$. We have then calculated the coupling strength (ϵ_j^{ac}) at some representative BZ edges in the a^*b^* reciprocal plane. For each branch, we have averaged the found ϵ_j^{ac}, and assumed a linear dependence on $|\mathbf{q}|$. The latter assumption is correct only in the small $|\mathbf{q}|$ limit.[34]

The most important single parameter characterizing the strength of electron-phonon coupling in the superconductivity mechanism is the dimensionless electron-phonon coupling constant λ.[34,35] This parameter is in turn related to the Eliashberg coupling function $\alpha^2(\omega)F(\omega)$:[35]

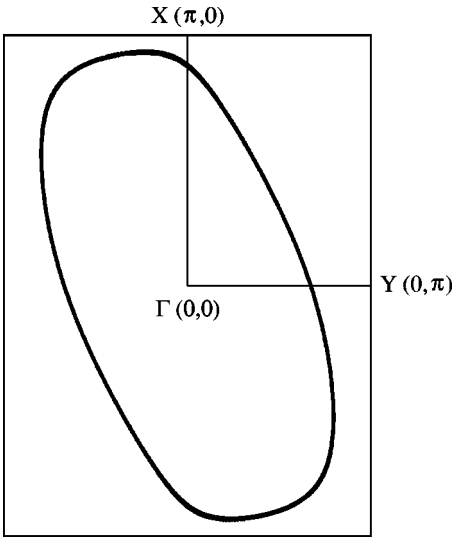

FIG. 1. β-(BEDT-TTF)$_2$I$_3$ Fermi surface on the a^*b^* reciprocal plane, calculated on the basis of the rectangular tight binding dimer model of Eq. (6).

$$\lambda=2\int_0^{\omega_{\max}}\frac{\alpha^2(\omega)F(\omega)}{\omega}d\omega, \tag{5}$$

where $F(\omega)$ is the phonon density of states per unit cell, and $\alpha^2(\omega)$ is an effective coupling function for phonons of energy ω. The *e-lph* Eliashberg coupling function can be evaluated from the QHLD phonon density of states and from the electron-phonon matrix element $g(\mathbf{k},\mathbf{k}';\mathrm{j})$ expressed in the reciprocal space[34]

$$\alpha^2(\omega)F(\omega)=N(E_F)\sum_j\langle|g(\mathbf{k},\mathbf{k}';j)|^2\delta(\omega-\omega_{\mathbf{q}j})\rangle_{\mathrm{FS}}, \tag{6}$$

where $\mathbf{q}=\mathbf{k}'-\mathbf{k}$,$\mathbf{k}$ and $\mathbf{k}'$ denoting the electronic wave vectors, and $N(E_F)$ is the density of states per spin per unit cell at the Fermi level. In Eq. (6), $\langle\ \rangle_{\mathrm{FS}}$ indicates the average over the Fermi surface.

We have calculated the g's in real space, as detailed above. In order to introduce the dependence on the electronic wave vector $\mathbf{k}$, as required in Eq. (6), we have to describe the electronic structure of the β-phase metal. To get a simple yet realistic model we make resort of the rectangular tight-binding dimer model,[36,37] where the BEDT-TTF dimers inside the unit cell are taken as a supermolecule. Actually, as in the κ phases, in the β phase the BEDT-TTF dimers are clearly recognized (in the present nomenclature, they are associated to the t_{AB} CT integral). In this model there is only one half-filled conduction band in the first BZ, whose dispersion relation as a function of the t_{KL} CT integrals is easily obtained (lettering of the CT integrals as in Ref. 22):

$$\epsilon(\mathbf{k})=t_{AB}+t_{AH}\cos(k_x)+t_{AE}\cos(k_y)+t_{AC}\cos(k_x+k_y). \tag{7}$$

The chemical potential is obtained numerically from the half-filling condition. The resulting Fermi surface on the a^*b^* plane is shown in Fig. 1. Although the BZ is different from the actual one, being referred to a rectangular lattice, the shape of the Fermi surface compares well with that avail-

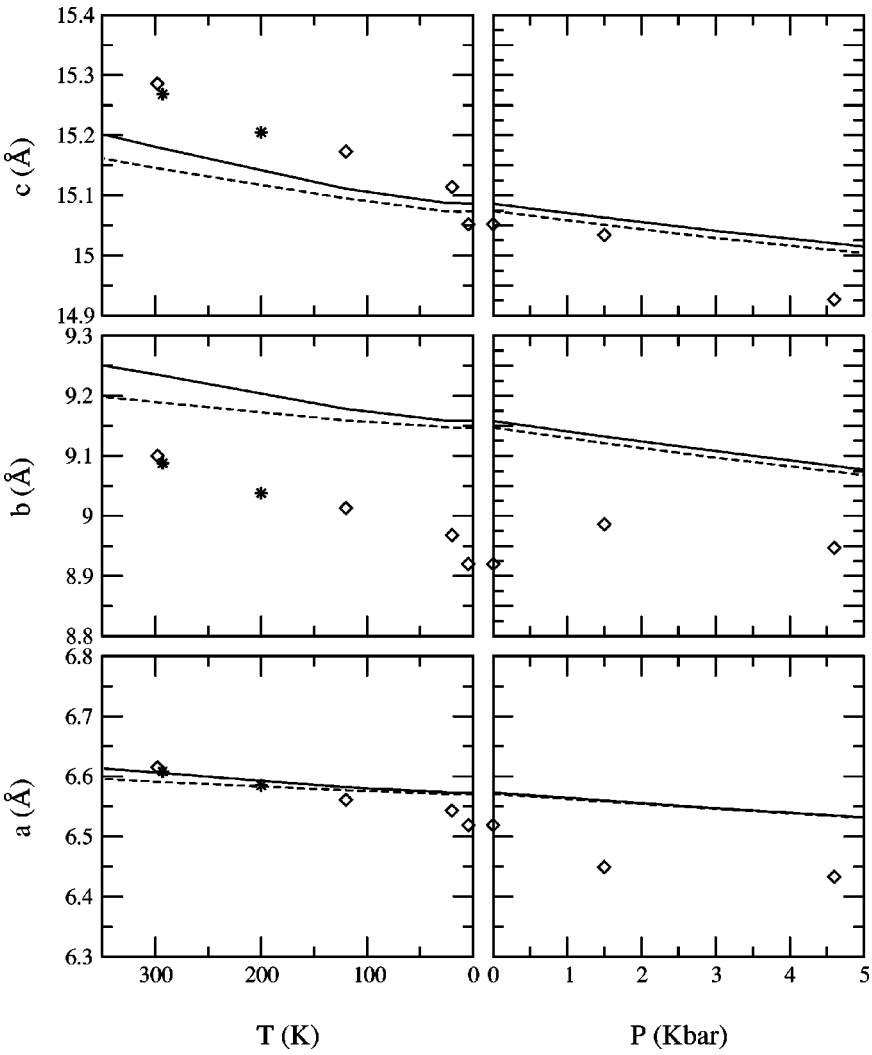

FIG. 2. Calculated and experimental crystallographics axis lengths of β-(BEDT-TTF)$_2$I$_3$ as functions of temperature and pressure. Full line: calculations taking into account the mixing between lattice and intramolecular modes. Dashed line: calculations within the rigid molecule approximation (RMA). The experimental points are taken from Refs. 23,27 (diamonds) and from Refs. 24,25 (asterisks).

able in the literature,[22] giving confidence to the use of the dimer model. Within tight-binding, the dependence in reciprocal space of the coupling constants associated to the interdimer (intercell) hoppings is given by[38]

$$g(\mathbf{k},\mathbf{k}';j)=2\mathrm{i}\,g(KL;\mathbf{q},j)[\sin(\mathbf{k}+\mathbf{q})\mathbf{R}-\sin\mathbf{k}\mathbf{R}], \quad (8)$$

where $\mathbf{R}$ represents the nearest-neighbor lattice vectors $(a,b,a+b)$, and $g(KL;\mathbf{q},j)$ are the corresponding real space intercell CT integrals. The Fermi surface reported in Fig. 1 is used to perform numerically the average of Eq. (6), yielding the interdimer contribution. The coupling constants associated with the modulation of the intradimer CT integral are treated as intramolecular coupling constants, and as such are independent of $\mathbf{k}$.[11,38] We finally remark that the *e-mv* Eliashberg coupling function is simply given by $[\alpha^2(\omega)F(\omega)]_{e\text{-}mv}=[N(E_F)/N]\Sigma_i g_i^2\delta(\omega-\omega_i)$, N being the number of molecules per unit cell and g_i being the usual *e-mv* coupling constant,[11] so that $\lambda_{e\text{-}mv}=N(E_F)E_{sp}^{mv}$.

III. RESULTS

A. Crystallographic structures

The unit cell of β-(BEDT-TTF)$_2$I$_3$ contains one I_3^- ion at the (0 0 0) inversion site and two BEDT-TTF molecules at generic sites.[22,23,27] At 4.5 K the two BEDT-TTF molecules have a boat geometry (with the terminal C atoms in 9a,10a positions) and are interconverted by the inversion.[23] At 120 K the lattice is disordered[27] and inversion symmetry is satisfied only statistically, with a mixture of boat and chair molecules.

In Fig. 2 we compare the experimental crystal axis lengths[23–25,27] as a function of T and p to the calculations performed first with RMA, and then by allowing for non rigid molecules with the addition of a subset of intramolecular modes, as explained in Sec. II D. It can be seen that the structures are only marginally affected by the RMA. A more detailed comparison between the experimental[23] and computed structures (with nonrigid molecules) is reported in Table II. All calculations have been performed by minimizing the free energy G with the molecules in their experimental, ordered geometry at 4.5 K.[23] To investigate the effect of small changes in molecular geometry, the structures of β-(BEDT-TTF)$_2$I$_3$ have been recomputed with the 120 K geometry[27] and ordered molecules (staggered or boat form). The effect of the change in molecular geometry is negligible. At all temperatures, β-(BEDT-TTF)$_2$I$_3$ appears to be thermodynamically more stable than α-(BEDT-TTF)$_2$I$_3$,[20] giving account for the irreversible interconversions of α-(BEDT-TTF)$_2$I$_3$ into β-like phases.

The effect of molecular deformations has also been investigated, within the RMA approximation, by testing several

TABLE II. Structural data of β-(BEDT-TTF)$_2$I$_3$ as a function of T (K) and p (GPa): experimental (Ref. 23) and computed unit cell axis a,b,c (Å), angles α, β, γ (degrees), and volume V (Å^3). The lattice is triclinic, space group $P\bar{1}$ (C_i^1), with $Z=1$.

T	p		a	b	c	α	β	γ	V
4.5	0	expt.	6.519	8.920	15.052	95.32	96.09	110.44	807.6
		calc.	6.573	9.158	15.086	93.94	95.04	111.83	834.7
20	0	expt.	6.543	8.968	15.114	95.34	96.05	110.30	819.1
		calc.	6.573	9.159	15.087	93.94	95.04	111.83	834.8
120	0	expt.	6.561	9.013	15.173	95.07	95.93	110.28	829.2
		calc.	6.582	9.178	15.111	93.79	95.01	111.75	839.9
298	0	expt.	6.615	9.100	15.286	94.38	95.59	109.78	855.9
		calc.	6.606	9.235	15.180	93.42	94.92	111.55	854.0
4.5	0.15	expt.	6.449	8.986	15.034	94.79	96.57	111.29	799.1
		calc.	6.560	9.132	15.063	94.02	95.10	111.83	829.1
6.1	0.46	expt.	6.433	8.947	14.927	95.15	96.77	111.40	786.1
		calc.	6.536	9.083	15.020	94.17	95.23	111.83	818.8

model geometries in β-(BEDT-TTF)$_2$I$_3$ as well as in α-(BEDT-TTF)$_2$I$_3$ phases. The potential energy has been minimized with the experimental geometries[27,39] and with chair-α, chair-β, boat-α, and boat-β model geometries. The chair-α geometry is the average of the two chair molecules in α-(BEDT-TTF)$_2$I$_3$,[39] while chair-β is the molecule of β-(BEDT-TTF)$_2$I$_3$ with all the terminal carbons in 9b,10b positions.[27] The boat-α and β geometries are those observed in the corresponding phases.[27,39] For both α and β phases, the potential energy minimum is found with experimental geometry of that phase, and the system becomes less stable if any other geometry is used. It should be noticed that for β-(BEDT-TTF)$_2$I$_3$ the boat-β geometry coincides with the experimental geometry at 4.5 K, and thus yields the lowest energy. The difference between α-(BEDT-TTF)$_2$I$_3$ and β-(BEDT-TTF)$_2$I$_3$ essentially vanishes if the chair-α and boat-α geometries are used in the β phase, while the chair-β and boat-β geometries drastically destabilize the α phase. This behavior clearly indicates that molecular deformations play a crucial role in determining the *relative* stability of various (BEDT-TTF)$_2$I$_3$ phases, but have a minor effect on the crystallographic structure *within* a given phase.

B. Specific heat and phonon assignment

We now turn our attention to the phonon structure. The number of bands experimentally observed in the low frequency (10–200 cm^{-1}) Raman and infrared spectra of β-(BEDT-TTF)$_2$I$_3$ is lower than expected, so that vibrational spectra do not offer a very stringent test for the calculated phonon frequencies. We therefore first make comparison to the experimental data available for the specific heat, which depends on the frequency distribution. Figure 3 shows that if we calculate the specific heat adopting the RMA, at 20 K the calculated C_V (dotted line) is about 50% smaller than the experimental C_p (dots, from Ref. 40). The difference between C_V and C_p is usually small for solids, since their thermal expansion is small. Therefore, we attribute most of the discrepancy between C_V and C_p to the intramolecular modes, which are neglected in the RMA calculation. Figure 3 also shows the C_V computed by relaxing the RMA, as specified in Sec. II D. The agreement between calculation and experiment is indeed greatly improved. We anticipate that the same kind of result has been obtained for κ-(BEDT-TTF)$_2$I$_3$.[43] These results clearly indicate that RMA *must* be relaxed in realistic calculations of the low-frequency phonons of BEDT-TTF crystals.

We next move to the characterization and assignment of individual low-frequency phonons. In the β phase we have only one formula unit in the triclinic unit cell, and below 220 cm^{-1} we expect Raman activity for eight lattice modes, nine BEDT-TTF intramolecular modes, and one stretching of I_3^-. In infrared we expect six lattice modes, nine BEDT-TTF intramolecular modes, and three I_3^- modes. Of course, the modes are actually mixed, as RMA is not applicable, but the number of $\mathbf{q}=0$ phonons remains the same. The calculated frequencies are compared with the experimental ones[6,32,44] in Tables III and IV for A_u and A_g modes, respectively. The comparison between calculated and experimental vibrational frequencies is satisfactory, although not very significant given the low number of observed frequencies. Since we also have all the corresponding eigenvectors, we report an ap-

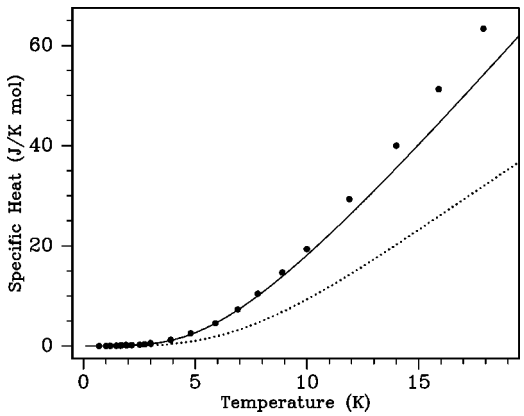

FIG. 3. Specific heat of β-(BEDT-TTF)$_2$I$_3$ as a function of T. Full line: computed C_V obtained from coupled lattice and intramolecular modes. Dotted line: computed C_V due only to lattice modes within the RMA approximation. The dots represent the experimental C_p, from Ref. 40.

TABLE III. Low-energy A_u phonons of β-(BEDT-TTF)$_2^+$I$_3^-$.

Expt.[a]	Calc.[b]	Approximate description			
		I_3^-(%)		BEDT-TTF$_2^+$(%)	
cm^{-1}	cm^{-1}	lattice	internal	lattice	internal
	216				98
	173				90
	151			26	68
133	148		86		10
130	136		8		88
124	123			48	48
	114			8	86
95	112			24	72
91	90			56	40
	84	8	13	34	44
	74		56	26	12
71	69			22	78
	67	8	40	18	36
	62	22	44	10	20
	57		23	44	28
48	43	55	11	26	
	33	44		22	30
	17	41		22	36

[a]From Ref. 32.

[b]The frequencies refer to the minimum *G* structure at 120 K. We have chosen this temperature since in this way we can compare the phonon frequencies and eigenvectors for the minimum *G* and the experimental structure (Ref. 27). The frequency differences between the two sets of calculations are quite small, so only the minimum *G* result is reported.

proximate description of the phonons, given for both BEDT-TTF and I_3^- as a percentage of the lattice (rigid molecule) and of the intramolecular contributions. Since in some cases there is a considerable mixing between lattice and molecular modes, a clear distinction cannot be made. Figure 4 reports the full dispersion curves along the C,V,X, and Y directions[22] and density of states of β-(BEDT-TTF)$_2$I$_3$. In order to make the figure more readable, we have limited the highest frequency to 150 cm^{-1}. Figure 4 puts in evidence the complex structure of β-(BEDT-TTF)$_2$I$_3$ low-frequency phonons. We have a very dense grouping of modes in the 50–100 cm^{-1} region, with several avoided crossings between the dispersion curves, and clear mixing between lattice and molecular modes. Only the acoustic phonon branches contribute to the density of states below $\sim$25 cm^{-1}, so that the typical ω^2 dependence is observed. On the other hand, at energies higher than $\sim$140 cm^{-1} the almost dispersionless intramolecular modes dominate, and the phonon density of states appears as a sum of deltalike peaks (not shown in the figure).

C. Electron-phonon coupling

The *e-lph* coupling constants for the optical phonons of β-(BEDT-TTF)$_2$I$_3$ are reported in Table IV. As explained in Sec. II, if one assumes that the eigenvectors are independent of **q**, only the A_g phonons can couple to electrons. In Table IV for each phonon we report both the individual $g(KL;j,\mathbf{q})$ [Eq. (4)] and the small polaron binding energy ϵ_j. The two most strongly coupled modes are those calculated at 32 and 113 cm^{-1}. Whereas the former mode has been observed in the Raman spectrum, and together with the lower frequency mode (27 cm^{-1}) undergoes a drastic intensity weakening at T_c,[6] the latter has not been reported even in the normal state.[6,44] The reason might be due to the proximity of the very intense, resonantly enhanced band at 121 cm^{-1}, due to the symmetric stretch of the I_3^- anion. One band at 107 cm^{-1} has been observed below 6 K for 488 nm laser excitation.[45] On the other hand, a band at 109 cm^{-1}, whose intensity varies with sample and irradiation, has been attributed to the splitting of the I_3^- stretching mode,[44] as a consequence of the commensurate superstructure reported in one x-ray investigation at 100 K.[39] Certainly the 100–130 cm^{-1} spectral region deserves further experimental scrutiny with the latest generation of Raman spectrometers. A second observation is that whereas the 113 cm^{-1} mode involves only the BEDT-TTF units, and is mostly a lattice mode, the 32 cm^{-1} one is a mixing between rigid I_3^- motion and ''flexible'' BEDT-TTF vibrations. This finding suggests a not marginal role of the counterion sheets in β-type BEDT-TTF salts.

As shown by Table IV, the coupling of individual optical modes with electrons is in general not particularly strong, but on the whole the strength of *e-lph* coupling, as measured by the sum of the ϵ_j, is appreciable, around 45 meV, to which we have to add the contribution of the acoustic phonons. For the sake of comparison, we give also the ϵ_j^{ac} for the three acoustic branches, calculated as average over several points at the BZ edges. In order of decreasing phonon frequency (see Fig. 4) the ϵ^{ac} are 2.3, 3.3, and 18.2 meV, respectively. The coupling strength of the lowest acoustic branch at the zone edge is comparable to that of the most strongly coupled optical phonons. Thus the overall *e-lph* coupling strength is of the same order of magnitude as that due to *e-mv* coupling, about 70 meV.[15]

We can make a more direct connection with superconducting properties by calculating the Eliashberg function and the dimensionless electron-phonon coupling constant λ. As seen in Eq. (6), the absolute value of the Eliashberg function depends on the electronic density of states at the Fermi energy $N(E_F)$. Experimental estimates of this critical parameter are problematic, since the measured quantities already include or the λ enhancement factor, or the Coulomb enhancement factor, or both. The available theoretical estimates for β-(BEDT-TTF)$_2$I$_3$ are all based on the EH tight binding method. It is known that this method underestimates the density of states. In particular, for κ phase BEDT-TTF superconducting salts the EH density of states is about 1.5 times smaller than that obtained by more sophisticated calculations.[37] We adopt the EH value $N(E_F)=2.1$ spin states/eV/unit cell,[46] keeping in mind that this constitutes a lower limit. To our advantage, we can compare the calculated $\alpha^2(\omega)F(\omega)$ with that derived from normal state current/voltage measurements at a point contact junction.[4,47] This kind of experiment is rather difficult to perform on organic crystals such as β-(BEDT-TTF)$_2$I$_3$, since one has to be careful about pressure effects at the point contact. The use of a contact between two β-(BEDT-TTF)$_2$I$_3$ crystals made

TABLE IV. Low-energy A_g phonons and coupling constants of β-(BEDT-TTF)$_2^+$I$_3^-$.

Expt.[a]	Calc.[b]	Approximate description				Coupling Constants (meV)[c]				
		I_3^-(%)		BEDT-TTF$_2^+$(%)						
cm^{-1}	cm^{-1}	lattice	internal	lattice	internal	$g(AB;j)$	$g(AC;j)$	$g(AE;j)$	$g(AH;j)$	ϵ_j(meV)[d]
214	207				90		−1	−1		
179	172				92		−1	−1		
	165			16	84	3		2	−1	
149	144			16	80	−1	2	1	−2	
	131			12	86	−6			1	
121	120		89			−3	1	1	−1	
	113			58	32	−13	7	3	−1	16
	111				90	−4	1	−1	3	
91	87	10		50	36	2		3	4	
	81			48	48	−1	−1	−1	−5	
	73			8	88	2		2	1	
	64			78	22	−4	6	−3	3	9
	60	33		18	50	1	−3	−4	5	7
53	51	25		50	22	4		−6	3	10
	49	20		66	14	4	−3	−1	2	
39	44	33		60		−1	−2	−2	2	
32	32	56		16	24	6	−2	−5	1	17
27	29	10		76	10	−4	4	2	2	11

[a]From Refs. 6,44.

[b]See note b of Table III.

[c]The modulated hopping integrals between dimers are labeled according to Ref. 22. The calculated equilibrium values are: $t_{AB}=0.22$ eV, $t_{AC}=0.08$ eV, $t_{AE}=0.10$ eV, $t_{AH}=0.06$ eV.

[d]Only values larger than 5 meV are reported.

the current-voltage characteristics rather stable, from which the $\alpha^2(\omega)F(\omega)$ function reported in the upper panel of Fig. 5 was obtained.[47] We have changed the scale on the ordinate axis to maintain the same energy unit (cm^{-1}) throughout. It is clear that the spectral resolution of the experiment is larger than ~ 10 cm^{-1}, and probably increases with energy. Indeed, no spectral detail is visible beyond 240 cm^{-1}, where the contribution of *e-mv* coupled modes should be

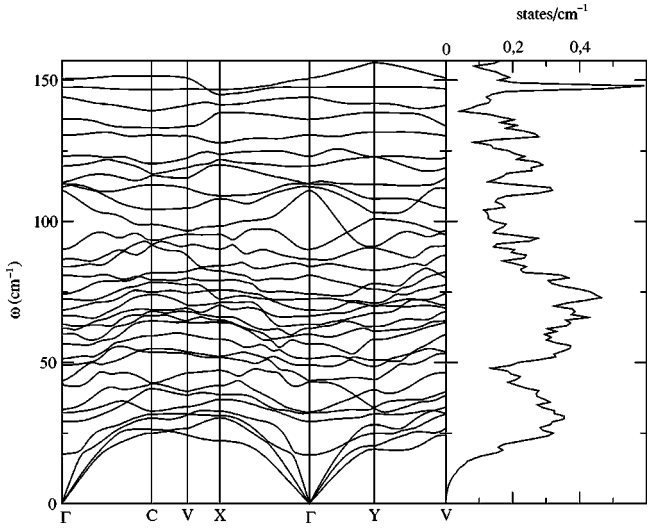

FIG. 4. Dispersion curves and density of states $F(\omega)$ of β-(BEDT-TTF)$_2$I$_3$ low-frequency phonons. The zone edges are labeled according to Ref. 22.

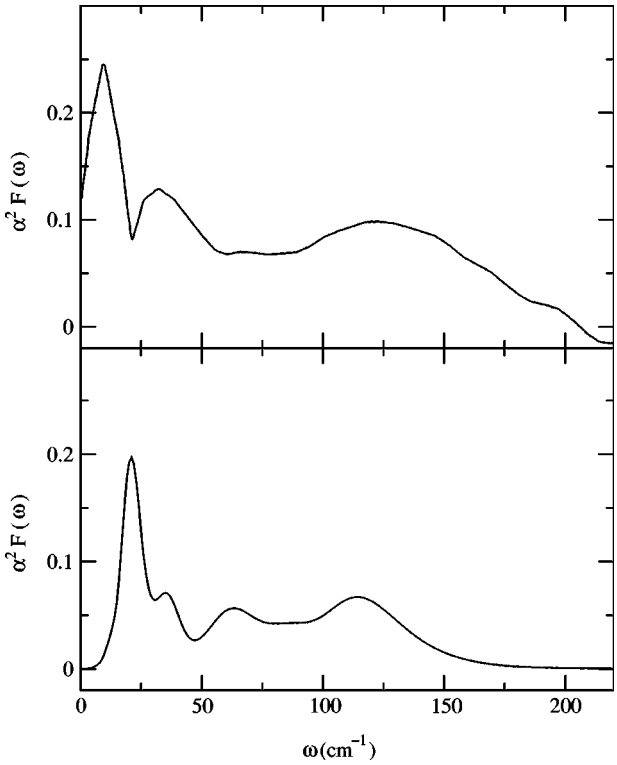

FIG. 5. Upper panel: the Eliashberg function as measured from point-contact tunneling experiments (adapted from Ref. 47). Lower panel: the calculated contribution to $\alpha^2(\omega)F(\omega)$ from low frequency *e-lph* coupled phonons.

detectable.[5] Therefore, to make easier the visual comparison with the experimental data, we have smoothed the calculated $\alpha^2(\omega)F(\omega)$ (Fig. 5, lower part) by a convolution with a Gaussian distribution. We have also assumed that the Gaussian distribution width increases linearly with ω (from 0.1 to 20 cm^{-1} in the 1–200 cm^{-1} interval).

Figure 5 puts in evidence the very good agreement between experiment and calculation. The absolute scale of $\alpha^2(\omega)F(\omega)$ turns out to be almost the same, even if both experiment and calculation are affected by the abovementioned uncertainties. The three main peaks observed in the experiment are well reproduced and are identified as due to the most strongly coupled phonon branches, namely, the lowest frequency acoustic branch and the optical phonons at 32 and 113 cm^{-1}. The calculated frequency of the prominent peak due to acoustic phonons is higher than the experimental one (22 vs 10 cm^{-1}). This discrepancy might be due to the fact that the experiment refers to the β_L-(BEDT-TTF)$_2$I$_3$) phase, whereas our calculation refers to a perfectly ordered phase such as the β*-(BEDT-TTF)$_2$I$_3$.[47] We also remark that, at variance with traditional superconductors, the Eliashberg function is remarkably different from the phonon density of states (Fig. 4). For instance, the peak around 120 cm^{-1} in $F(\omega)$ is due to the dispersionless I_3^- stretching mode, which is completely decoupled from the electron system, whereas the broad peak in $\alpha^2(\omega)F(\omega)$ is due to the nearby (113 cm^{-1}) ''lattice'' mode of the BEDT-TTF molecules. Due to the complex phonon structure, $\alpha^2(\omega)$ is not nearly constant, but varies rapidly with the frequency.

The dimensionless coupling constant λ obtained by integration of $\alpha^2(\omega)F(\omega)/\omega$ up to 240 cm^{-1} turns out to be around 0.4. The contribution to λ from *e-mv* coupled modes,[15] computed by $\lambda_{e\text{-}mv}=N(E_F)E_{sp}^{mv}$, is instead around 0.1. Thus in the McMillan picture[11] the overall λ of β-(BEDT-TTF)$_2$I$_3$ is $\sim$0.5, which may well account for the observed $T_c=8.1$ K.[47]

IV. DISCUSSION AND CONCLUSIONS

The computational methods we have adopted to analyze the crystal and lattice phonon structure, and the electron-phonon coupling strength of β-(BEDT-TTF)$_2$I$_3$ are empirical or semiempirical. The form of QHLD atom-atom potentials has no rigorous theoretical justification, and the corresponding parameters are derived from empirical fittings. Also the EH method we have used to characterize the β-(BEDT-TTF)$_2$I$_3$ electronic structure is semiempirical, albeit with an experimental basis far wider than QHLD. In view of the obvious limitations of empirical or semiempirical methods, the success achieved in the case of β-(BEDT-TTF)$_2$I$_3$ is even beyond our expectations, also considering that *none* of the empirical parameters has been adjusted to fit β-(BEDT-TTF)$_2$I$_3$ experimental data.

Indeed, *all* the available β-(BEDT-TTF)$_2$I$_3$ experimental data have been accounted for. The crystal structure, and its variation with T and p, is correctly reproduced (Fig. 2 and Table II). Useful hints about the relative thermodynamic stability of α and β phases has been obtained, as well as some indications on the effect of BEDT-TTF conformation on the phase stability. The specific heat (Fig. 3) and the few detected Raman and infrared bands have been accounted for by including the coupling with low-frequency molecular vibrations. Finally, the point contact Eliashberg spectral function has been satisfactorily reproduced (Fig. 5).

Despite the success, it is wise to keep in mind the QHLD limitations. First and foremost, conformational disorder in the crystal structure is not included. This is not a limitation of the QHLD method only, but it is a serious one particularly for β-(BEDT-TTF)$_2$I$_3$ salts, where disorder plays an important role even in the superconducting properties. It is in fact believed that a fully ordered structure is at the origin of the higher T_c (8.1 K) displayed by β* or β_H phases with respect to β_L-(BEDT-TTF)$_2$I$_3$ (1.5 K).[23] Furthermore, even if the QHLD method is able to follow the T and p dependence of the crystal structure, phase transitions implying subtle structural changes may be beyond its present capabilities, even for fully ordered structures. The relative stabilities of the phases can indeed be reproduced only at a qualitative level. For what concerns the electron-phonon coupling constants, one has to keep in mind that these depend on QHLD phonon eigenvectors, which are obviously more prone to inaccuracies than the calculated phonon energies. Finally, extension to other BEDT-TTF salts with counterions different from I_3^- is not obvious, requiring additional atom-atom parameters.

Once the above necessary words of caution about the method are spelled out, we can underline what in any case we have learned from the present QHLD calculations. So far, in the lack of any description, no matter how approximate, of the phonons modulating the CT integrals, only speculative discussions about their role in the superconductivity could be put forward, catching at best only part of the correct picture. One of the most important indications coming out from the present paper is the need of relaxing the RMA. So from one hand we cannot try to focus on the isolated molecule intramolecular vibrations presumably modulating the CT integral,[28] and on the other hand referring to ''librations'' of the rigid molecules[4] lacks of precise meaning. In other words, there is no simple or intuitive picture of the phonons modulating the CT integrals. Our results, and the overall mode mixing, suggest that also the counterions vibrations might play some role in the coupling.

The results presented here definitely assess the very important role played by the low-frequency phonons in the superconducting properties of BEDT-TTF salts. *Both* acoustic and optic modes modulating the CT integral are involved. The overall dimensionless coupling constant is $\sim$0.4, much larger then that due to *e-mv* coupled phonons ($\sim$0.1). Of course, a mere numerical comparison of the two λ's is not particularly significant, since one has to keep in mind the very different time scales (frequencies) of the two types of phonons. The phonons appreciably modulating the CT integrals fall in the 0–120 cm^{-1} spectral region (Table IV), whereas those modulating on-site energies have frequencies ranging from 400 to 1500 cm^{-1}.[15] Applicability of the Migdal theorem to the latter appears dubious: nonadiabatic corrections[48] or alternative mechanisms such as polaron narrowing[49] have been suggested. For these reasons we will not get involved into detailed discussions about the relative role of *e-lph* and *e-mv* coupling in the superconductivity mechanism. We limit ourselves to state that phonon medi-

ated coupling can well account for the observed critical temperature of the ordered β-(BEDT-TTF)$_2$I$_3$ phase, given plausible values of the other fundamental parameter, the Coulomb pseudopotential μ.[11,47]

The results of the present paper suggest that phonon mediated mechanism is responsible for the superconductivity of BEDT-TTF-based salts. Analogous conclusion was reached on the basis of the solution of the BCS gap equation for κ phase BEDT-TTF salts,[36] and high resolution specific heat measurements have been interpreted in terms of strong coupling BCS theory.[50] On the other hand, evidences are also accumulating towards nonconventional coupling mechanisms in organic superconductors such as spin-fluctuation mediated superconductivity.[51] Similar apparently contrasting experimental evidences are also found for cuprates,[52] pointing to a superconductivity mechanism where *both* electron-phonon coupling and antiferromagnetic spin correlations are taken into account.

ACKNOWLEDGMENTS

We express many thanks to Rufieng Liu for providing the *ab initio* Cartesian displacements of BEDT-TTF, to R. Swietlick for sending us unpublished Raman spectra of β-(BEDT-TTF)$_2$I$_3$, and to A. Müller for useful correspondence. We acknowledge helpful discussions with many people, notably A. Painelli, D. Pedron, D. Schweitzer, H. H. Wang, and J. Wosnitza. This work has been supported by the Italian National Research Council (CNR) within its ''Progetto Finalizzato Materiali Speciali per tecnologie Avanzate II,'' and the Ministry of University and of Scientific and Technological Research (MURST).

[1] A.J. Berlinsky, J.F. Carolan, and L. Weiler, Solid State Commun. **15**, 795 (1974).
[2] K. Yamaji, Solid State Commun. **61**, 413 (1987).
[3] H. Gutfreund, C. Hartzstein, and M. Weger, Solid State Commun. **36**, 647 (1980).
[4] A. Nowack, M. Weger, D. Schweitzer, and H.J. Keller, Solid State Commun. **60**, 199 (1986).
[5] T. Ishiguro, K. Yamaji, and G. Saito, *Organic Superconductors*, 2nd ed. (Springer, Heidelberg, 1998).
[6] K.I. Pokhodnia, A. Graja, M. Weger, and D. Schweitzer, Z. Phys. B: Condens. Matter **90**, 127 (1993).
[7] D. Pedron, G. Visentini, E. Cecchetto, R. Bozio, J.M. Williams, and J.A. Schlueter, Synth. Met. **85**, 1509 (1997); D. Pedron, G. Visentini, R. Bozio, J.M. Williams, and J.A. Schlueter, Physica C **276**, 1 (1997).
[8] J.E. Eldridge, Y. Lin, H.H. Wang, J.M. Williams, and A.M. Kini, Phys. Rev. B **57**, 597 (1998).
[9] V. Merzhanov, P. Auban-Senzier, C. Bourbonnais, D. Jérome, P. Batail, J. -P. Buisson, and S. Lefrant, C. R. Acad. Sci. Paris **314**, 563 (1992).
[10] A.M. Kini, K.D. Carlson, H.H. Wang, J.A. Schlueter, J.D. Dudek, S.A. Sirchio, U. Geiser, K.R. Lykke, and J.M. Williams, Physica C **264**, 81 (1996), and references therein.
[11] D. Pedron, R. Bozio, M. Meneghetti, and C. Pecile, Mol. Cryst. Liq. Cryst. **234**, 161 (1993).
[12] J.E. Eldridge, C.C. Homes, J.M. Williams, A.M. Kini, and H.H. Wang, Spectrochim. Acta, Part A **51**, 947 (1995).
[13] E. Demiralp, S. Dasgupta, and W.A. Goddard III, J. Phys. Chem. A **101**, 1975 (1997).
[14] R. Liu, X. Zhou, and H. Kasmai, Spectrochim. Acta **53**, 1241 (1997).
[15] G. Visentini, M. Masino, C. Bellitto, and A. Girlando, Phys. Rev. B **58**, 9460 (1998).
[16] W. Ludwig, *Recent Developements in Lattice Theory*, Vol. 43 of Springer Tracts in Modern Physics (Springer-Verlag, Berlin, 1967).
[17] R.G. Della Valle, E. Venuti, and A. Brillante, Chem. Phys. **202**, 231 (1996).
[18] A.J. Pertsin and A.I. Kitaigorodsky, *The atom-atom potential method*, Vol. 43 of Springer Series in Chemical Physics (Springer-Verlag, Berlin, 1987).
[19] A. Brillante, R.G. Della Valle, G. Visentini, and A. Girlando, Chem. Phys. Lett. **274**, 478 (1997).
[20] R.G. Della Valle, A. Brillante, G. Visentini, and A. Girlando, Physica B **265**, 195 (1999).
[21] E.B. Yagubskii, I.F. Shchegolev, V.N. Laukhin, P.A. Kononovich, M.V. Kartsovnic, A.V. Zvarykina, and L.I. Bubarov, JETP Lett. **39**, 12 (1984).
[22] T. Mori, A. Kobayashi, Y. Sasaki, H. Kobayashi, G. Saito, and H. Inokuchi, Chem. Lett. **1984**, 957. In this paper the *a* and *c* crystallographic axes are interconverted with respect to the conventional choice. The labeling of the BZ edges have to be changed accordingly, with *X* replacing *Z*. See T. Mori and H. Inokuchi, J. Phys. Soc. Jpn. **57**, 3674 (1988).
[23] A.J. Schultz, H.H. Wang, and J.M. Williams, J. Am. Chem. Soc. **108**, 7853 (1986).
[24] H. Müller, S.O. Svensson, A.N. Fitch, M. Lorenzen, and D.G. Xenikos, Adv. Mater. **9**, 896 (1997).
[25] H. Müller, A.N. Fitch, M. Lorenzen, S.O. Svensson, S. Wanka, and J. Wosnitza, Adv. Mater. **11**, 541 (1999).
[26] D. Madsen, M. Burghammer, S. Fiedler, and H. Müller, Acta Crystallogr., Sect. B: Struct. Sci. **55**, 601 (1999).
[27] P.C.W. Leung, T.J. Emge, M.A. Beno, H.H. Wang, J.M. Williams, W. Petricek, and P. Coppens, J. Am. Chem. Soc. **107**, 6184 (1985).
[28] E. Demiralp, S. Dasgupta, and W.A. Goddard III, J. Am. Chem. Soc. **117**, 8154 (1995).
[29] S. Califano, V. Schettino, and N. Neto, *Lattice Dynamics of Molecular Crystals* (Springer Verlag, Berlin, 1981).
[30] E. Demiralp and W.A. Goddard III, J. Phys. Chem. **98**, 9781 (1994).
[31] D. Hall and D.E. Williams, Acta Crystallogr., Sect. A: Cryst. Phys., Diffr., Theor. Gen. Crystallogr. **31**, 56 (1975).
[32] M. Dressel, J.H. Eldridge, J.M. Williams, and H.H. Wang, Physica C **203**, 247 (1992).
[33] A. Fortunelli and A. Painelli, Phys. Rev. B **55**, 16 088 (1997).
[34] P.B. Allen and B. Mitrovic, Solid State Phys. **37**, 1 (1982).
[35] *Superconductivity*, edited by R.D. Parks (Dekker, New York, 1969), Vols. 1 and 2.
[36] G. Visentini, A. Painelli, A. Girlando, and A. Fortunelli, Europhys. Lett. **42**, 467 (1998).
[37] J. Merino and R. McKenzie, Phys. Rev. B **62**, 2416 (2000).

[38] E.M. Conwell, Phys. Rev. B **22**, 1761 (1980).
[39] H. Endres, H.J. Keller, R. Swietlik, D. Schweitzer, K. Angermund, and C. Krüger, Z. Naturforsch. A **41**, 1319 (1986).
[40] G.R. Stewart, J. O' Rourke, G.W. Crabtree, K.D. Carlson, H.H. Wang, J.M. Williams, F. Gross, and K. Andres, Phys. Rev. B **33**, 2046 (1986).
[41] R.M. Lynden-Bell, R. Kosloff, S. Ruhman, D. Danovich, and J. Vala, J. Chem. Phys. **109**, 9928 (1998).
[42] R. Liu (private communication).
[43] A. Girlando, M. Masino, R. G. Della Valle, A. Brillante, and E. Venuii (unpublished).
[44] R. Swietlik, D. Schweitzer, and D. Keller, Phys. Rev. B **36**, 6881 (1987).
[45] R. Swietlik (private communication).
[46] R.C. Haddon, A.P. Ramirez, and S.H. Glarum, Adv. Mater. **6**, 316 (1994).
[47] A. Nowack, U. Poppe, M. Weger, D. Schweitzer, and H. Schwenk, Z. Phys. B: Condens. Matter **68**, 41 (1986).
[48] L. Pietronero and S. Strässler, Europhys. Lett. **18**, 627 (1992).
[49] D. Feinberg, S. Ciuchi, and F. de Pasquale, Int. J. Mod. Phys. B **4**, 1317 (1990).
[50] H. Elsinger, J. Wosnitza, S. Wanka, J. Hagel, D. Schweitzer, and W. Strunz, Phys. Rev. Lett. **84**, 6098 (2000).
[51] J.M. Schrama, E. Rzepniewski, R.S. Edwards, J. Singleton, A. Ardavan, M. Kurmoo, and P. Day, Phys. Rev. Lett. **83**, 3041 (1999).
[52] D.J. Scalapino, Phys. Rep. **250**, 329 (1995), and references therein.